reconditioned. Therefore, the retained strength report herein for 288°C assumes less than a 5 minute exposure to that temperature.

Relationships were derived to model the effect of strength loss on both the immediate and reconditioned samples. The immediate tensile strength loss model is:

$$TS = 103.0 - 0.26T_c \tag{6}$$

where: TS = percent of original tensile strength
T_c = temperature in celsius

This model is linear and predicts retained strength of 58.8% at 170°C, whereas, Schaffer predicts a retained strength of 92%. Ostman [21] suggests that this discrepancy is due to the difference in moisture content between the test samples. Above 170°C it was speculated that all the water which was present during conditioning quickly evaporated. More closely related, the model and Schaffer both report a retained strength, after cooling, of 27-28% of the original strength.

The immediate strength loss associated with compressive failure is linear, in the form:

$$CS = 106.2 - 0.29T_c \tag{7}$$

where: CS = percent of original compressive strength
T_c = temperature in degrees celsius.

This model predicts a retained strength of 22.7% at a temperature of 288°C, compared to Schaffer's reported 15%.

Kundsen and Schniewind reported on the reconditioned strength of wood samples in both tension and compression. Generally, the tensile samples failed to regain much of their original strength. The model as expressed is described as a second order equation, in the form of:

$$TS = 92.9 + 0.16T_c - 0.00116T_c^2 \quad (8)$$

where: TS = percent of original tensile strength
T_c = temperature in degrees celsius.

The reconditioned compressive sample actually demonstrated an increase of 5% at 160°C or 105% of the original strength. When reconditioned after reaching 288°C, 92% of room temperature strength was achieved. The model takes the form:

$$CS = 92.5 + 0.20T_c - 0.0007T_c^2 \quad (9)$$

where: CS = percent of original compressive strength
T_c = temperature in degrees celsius.

2.3. Illustration of Knudson and Schniewind equations.

The equations developed by Knudson and Schniewind are recommended for design purposes in ASCE *Structural Fire Protection* [22]. Since these equations represent the state-of-the-art, their use by design professionals is appropriate when evaluating heated or reconditioned wood elements. Table 2.1 shows the results of applying equations (6),

(7), (8) and (9) at a number of temperatures. As previously stated, the percentage of strength retained at 288°C is only applicable to wood exposed to that temperature for less than 5 minutes. The general practice is to ignore any contribution to strength from fibers which have reached this temperature. Graphical presentation of Table 2.1 shows tensile strength in Graph 2.1 and for compression strength in Graph 2.2.

TABLE 2.1

PERCENTAGE (%) OF ORIGINAL STRENGTH FOLLOWING EXPOSURE TO ELEVATED TEMPERATURE					
Temperature		Tensile Strength		Compressive Strength	
°C	°F	Immediate	Recon.	Immediate	Recon.
25	77	97%	93%	99%	97%
75	167	84	88	85	104
125	257	71	77	70	106
175	347	58	60	55	106
225	437	45	38	41	102
288	550	28	43	23	92

Knudson and Schniewind compared the mathematical models to actual fire test results presented by Dorn and Egner [23] for beams. Overall, the predicted sustainable loads at failure were within 30% of the actual loads, and predicted strength loss was within 7% of the actual strength loss. The error is more significant in the reconditioned beams and the authors suggest further study is necessary, prior to using the models in engineering analysis.

Similarly, column tests performed by Malhotra and Rogowski [24] were compared to the models. Again, predicted failure loads were within 37% of actual loads and predicted strength loss was within 8% of actual strength loss.

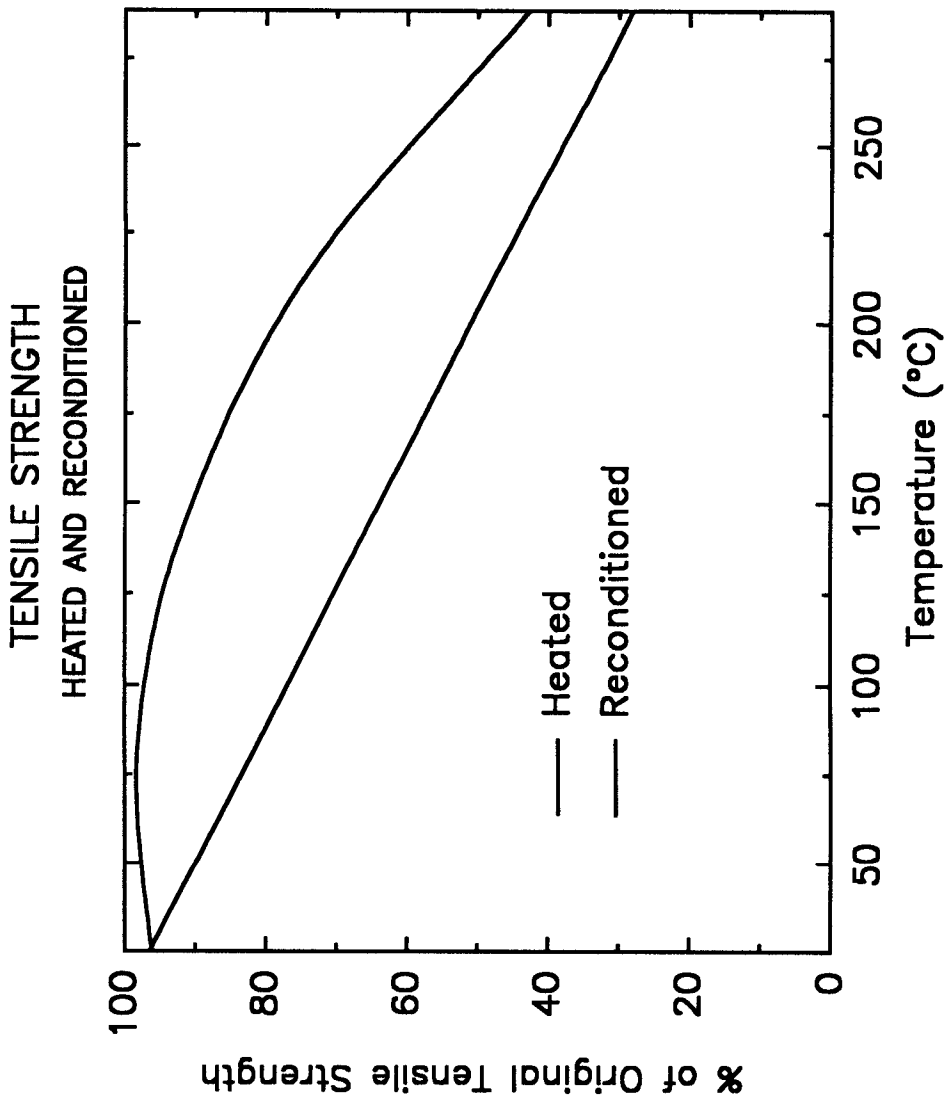

Figure 2.1 Intermediate and reconditioned tensile strength.

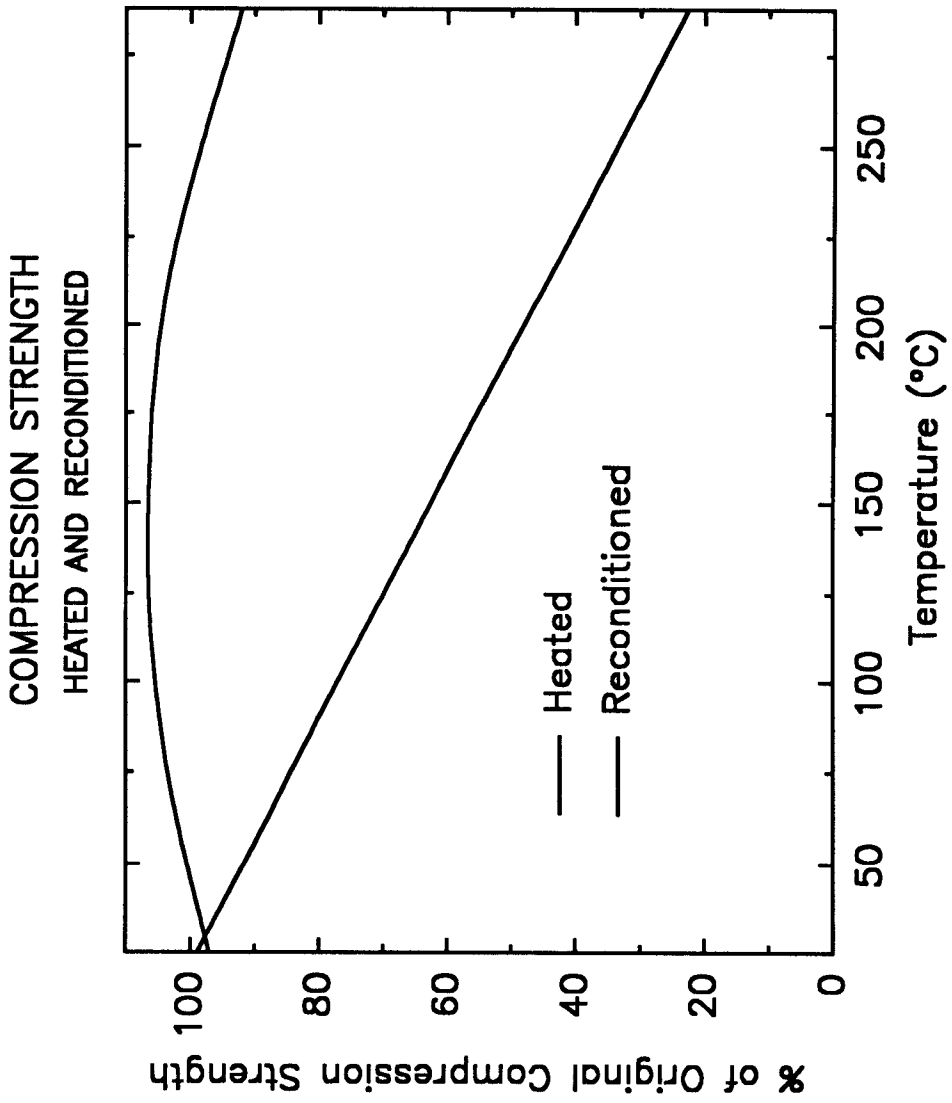

Figure 2.2 Intermediate and reconditioned compression strength.

CHAPTER 3

CHARRING

3.1 Introduction.

The Forest Products Laboratory (FPL), *Wood Handbook: Wood as an Engineering Material* states, "when wood is exposed to the ASTM E 119 fire test, it will char at the rate of 1/30 inch per minute for the first 8 minutes following ignition. Thereafter, the char layer has an insulating effect, and the rate decreases to 1/40 inch per minute. Considering the initial ignition delay, the fast initial charring, and then the slowing down to a constant rate, the average constant-charring rate is about 1/40 inch per minute or 1-1/2 inches per hour (Douglas-fir, 7 percent moisture content)." Although this is a simplified approximation of a very complex phenomenon, it has gained acceptance by scientists, fire investigators and building officials.

In a literature review by Schaffer [25] reports that four important parameters can control the charring rate of wood. They are: 1) density, 2) permeability along the grain, 3) moisture content and 4) thickness. Research by White [26] has shown that 1) and 3) are the most significant variables in approximating charring rates.

3.2. Empirical charring rate models.

Schaffer [27] evaluated large slabs of wood for one dimensional charring. Fire

exposure to beams and columns cause charring of three or four faces, depending on the framing detail. The more sides of the structural element which are subjected to the fire environment, the quicker the cross-section will absorb energy. Schaffer's work used a laminated slab to simulate one-dimensional charring. The one dimensional slab was chosen to model a beam with a minimum dimension of at least 6 inches. The influence of fire exposure and heat transfer from the opposing parallel face of a beam was considered insignificant for the first hour of exposure. This assumption has raised questions about the validity of the results for use in modeling. 2" thick dimension lumber will experience heat transfer from at least three faces if the element is unprotected.

Three wood species were tested to determine char rates transverse to the grain; Douglas-fir, southern pine and white oak, fabricated as 10" x 20" x 3" slabs. Prior to testing, the laminated slabs were conditioned to initial moisture contents of 6%, 12% and 18%. The test results from three constant furnace temperatures of 1000°F, 1500°F and 1700°F, were used in the derivation of the mathematical models.

3.2.1. Constant temperature exposure.

Schaffer developed two equations based on empirical results which predict the elapsed time of fire exposure and the rate of charring. The expression for the frequency factor, A, with the values of a, b, c and JE/R as given in Table 3.1 is:

$$A = (a + bM)\,\rho + c \tag{10}$$

where: M = moisture content
ρ = density

The equation for elapsed time to apparent char depth:

$$t = -A\ln\left(1-\frac{x}{3.0}\right)\exp\left[\frac{JE}{RT}\right] \tag{11}$$

where: J = Joule's constant
E = activation energy
R = gas constant
T = constant furnace temperature (K)

and for the charring rate, v (in/min):

$$v = \frac{1}{A}(3.0-x)\exp\left[\frac{JE}{RT}\right] \tag{12}$$

where: x = apparent char depth in inches from the surface

3.2.2. ASTM E 119 exposure.

Schaffer reviewed the work of Vorreiter [28] and found that his research compared favorably to the char depth vs. time data of specimens subjected to the ASTM E 119-61 standard fire test. This work resulted in the linear relationship shown in Equation 13 between time and char rate, when exposed to the standard time-temperature curve.

$$t = Bx \tag{13}$$

where: B = coefficient incorporating specific gravity
x = char layer depth

Schaffer was able to develop a new relationship for B based on the results of his testing. The regression constants are given in Table 3.1. Equation 14 is used to calculate the value of B for use in equation 13.

$$B = 2\{(a + bM)\rho + c\} \tag{14}$$

where: ρ = dry specific density
M = moisture content (%)

TABLE 3.1

SPECIES CONSTANTS FOR CHAR DEVELOPMENT EQUATIONS				
Species	Regression constants			JE/R (°K)
	a	b	c	
ASTM E119 Conditions				
Douglas-fir	28.726	0.578	4.187	NA
Southern pine	5.832	0.120	12.862	NA
White oak	20.036	0.403	7.519	NA
Constant Exposure Temperatures				
Douglas-fir	28.576	0.576	4.548	1,564
Southern pine	7.587	0.153	9.000	1,744
White oak	19.563	0.394	7.789	1,739

Schaffer estimates the accuracy of equations (11) and (13) to be between 2.6 and 5.1 minutes. The time of 2.6 minutes is the standard deviation of actual to predicted char depth under ASTM E 119 fire exposure. The larger standard deviation of 5.1 minutes is the worst case differential for constant temperature fire exposure. In general, Schaffer reported that the error increases with increasing depth of char. As a result of Schaffer's work, 288°C (550°F) has become a reference temperature for locating the base of the char layer. Due to the low thermal conductivity of wood, the temperature gradient within the slab is steep. As an example, at an inward distance of 1/4" from the 288°C char base layer, the temperature is a maximum of 182°C. In European practice, the reference temperature for locating the base of the char layer is 300°C, which is equally acceptable for research.

The charring rate caused by the ASTM E 119 fire exposure is of most interest to the practicing engineer. Graphs 3.1, 3.2 and 3.3 demonstrate the affect of various moisture contents on the charring rates of Douglas-Fir, southern pine and white oak based upon Equation (13). The dry specific density used in the development of the graphs are; $\rho = 0.48$ for Douglas-fir, $\rho = 0.51$ for southern pine (loblolly) and $\rho = 0.68$ for white oak.

Solid wood charring rate, as reported by White [26], is affected by a number of characteristics, such as, density, moisture, permeability, chemical composition and anatomy. The general conception that the greater the density of the species, the slower the charring rate is, for most cases, true. An exception is Western hemlock, when compared to Scots pine, both having a density of 0.545 gm/cc at 15% m.c. In a

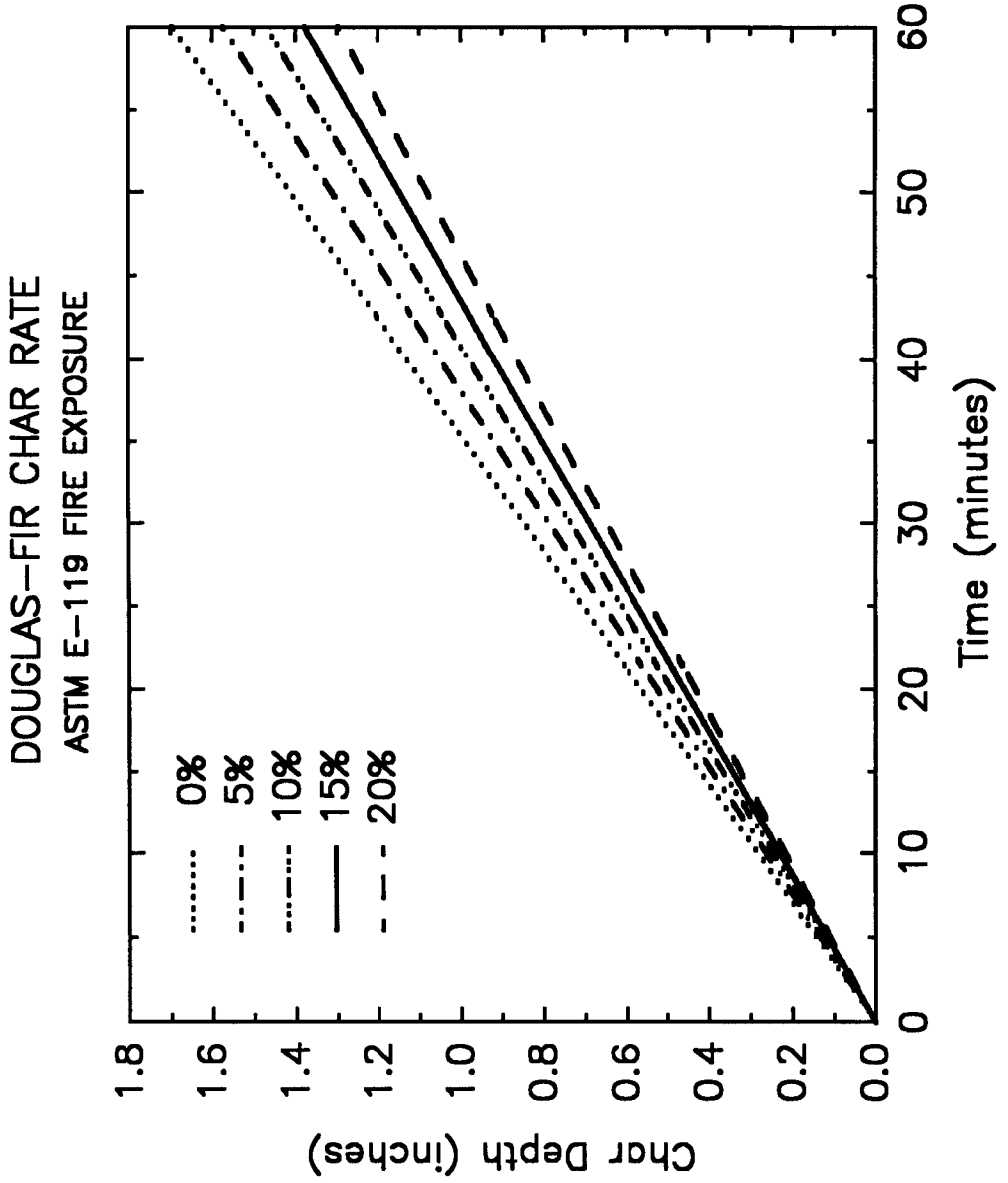

Figure 3.1 Douglas-fir char rate by Schaffer based on ASTM E 119 exposure at various moisture contents.

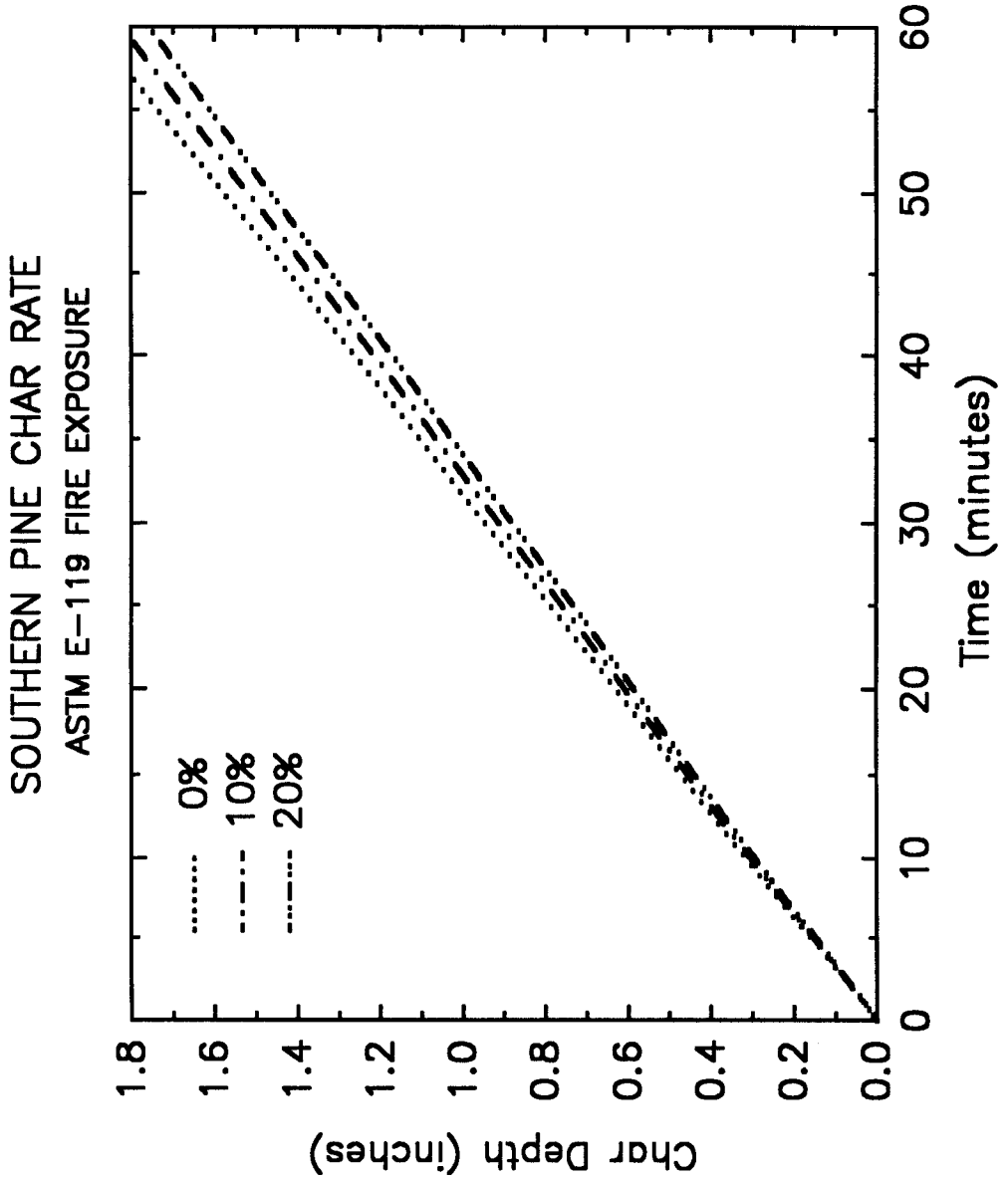

Figure 3.2 Southern Pine char rate by Schaffer based on ASTM E 119 exposure at various moisture contents.

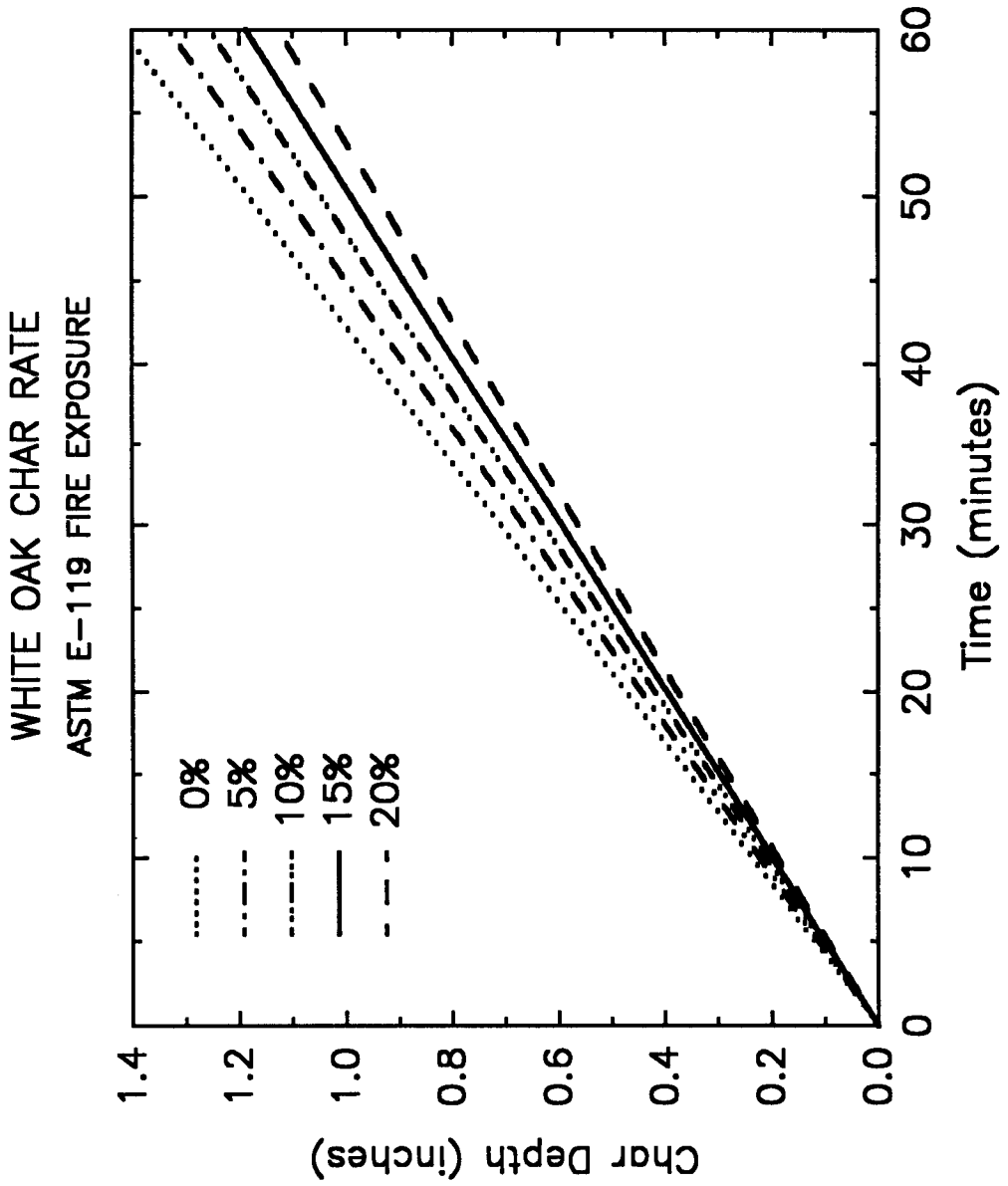

Figure 3.3 White oak char rate by Schaffer based on ASTM E 119 exposure at various moisture contents.

laminated test specimen, the Western hemlock charring rate is 30% faster parallel to the lamination and 14% faster perpendicular to the lamination (Rogowski [29], Malhotra and Rogowski [24]). The moisture movement in wood during pyrolysis has been shown to affect the charring rate. Research by White and Schaffer [30] suggests that the maximum moisture content occurs when the wood temperature is 100°C. As would be expected, the temperature profile of the cross section decreases as the distance from the surface increases. Permeability is believed also to affect the charring rate. Since moisture movement is critical, those species with poor permeability have slower char rates than species with good permeability. At 20% MC, southern pine, which readily accepts a pressure treatment, has a charring rate approximately 1.59 times that of Douglas-fir., which requires incising when treated [27].

White evaluated four probable models for the time dependant location of 288°C in the specimen, when exposed to an ASTM E 119 standard fire curve. A single parameter model of:

$$t = mx_c^{1.23} \tag{15}$$

or

$$\ln t = 1.23 \ln x_c + \ln m \tag{16}$$

where: t = time (min)
m = reciprocal of the char rate (min/mm)

x_c = char depth measured from original surface

was presented. The value of the parameter, m, varied for each species tested and for the relative humidity at which the specimen was conditioned.

White and Nordheim [31], further identified the significant variables associated with the value of m in equations 15 and 16. Two new variables are introduced in an effort to better describe the char rate. A hardwood/softwood classification values of (-1) and (+1), respectively, is identified by the factor, c. Additionally, the factor, d, was introduced to describe the treatability of the species in terms of penetration of a common preservative treating chemical, Chromated Copper Arsenate, CCA. Depth of penetration is related to transverse grain permeability of the species. The final model for m takes the form:

$$m = 0.162 + 0.809p + 0.0107u + 0.0689c - 0.00655pd - 0.00240cd \tag{17}$$

where:
- m = reciprocal of char rate
- p = oven-dry density or specific gravity
- u = percentage moisture content
- c = hardwood /softwood classification
- d = depth of CCA penetration

Mikkola [32] derives a simplified model to calculate charring rates and further develops relationships for each of the parameters. The simplified equation takes the

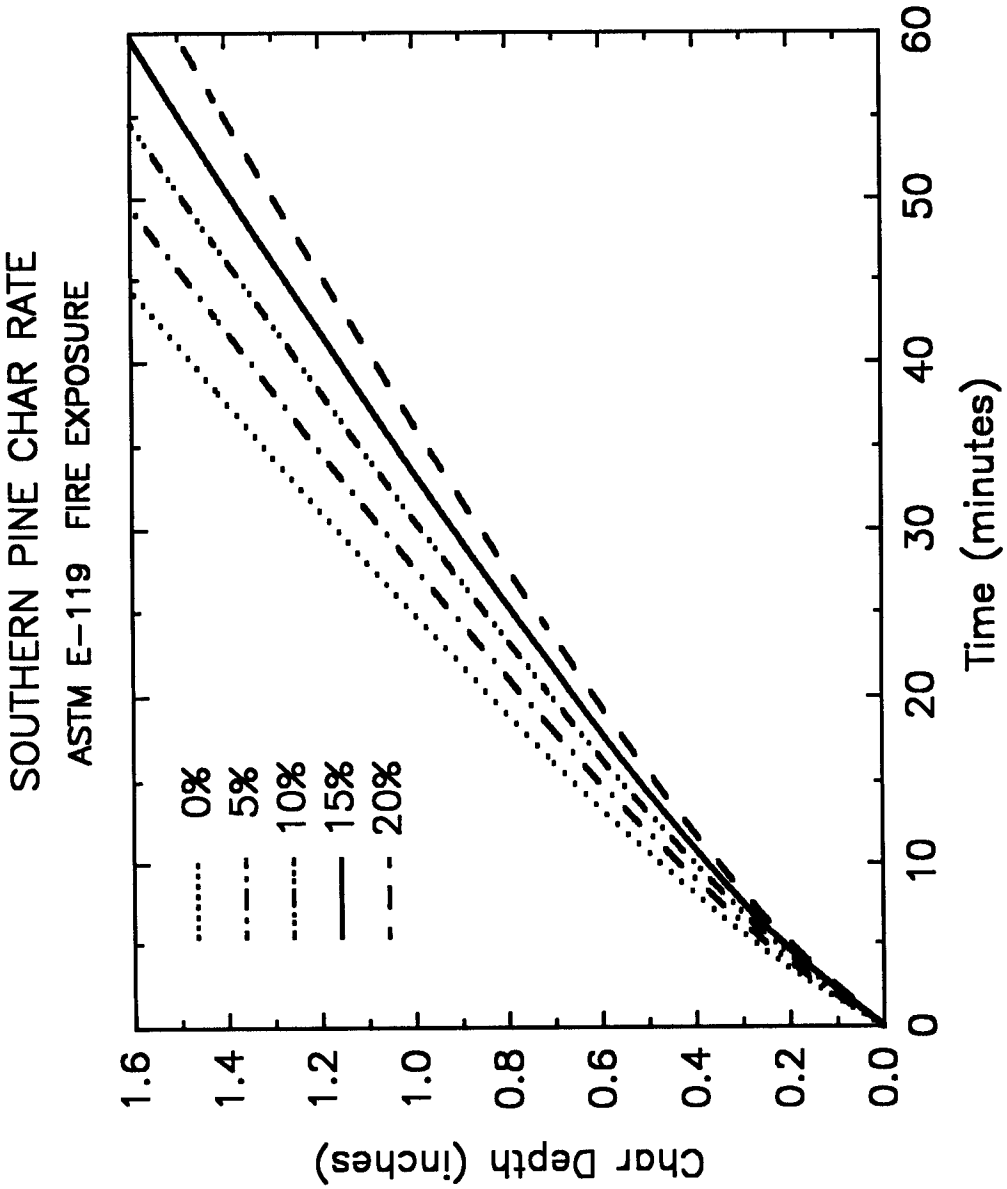

Figure 3.4 Southern pine char rate by White based on ASTM E 119 exposure at various moisture contents.

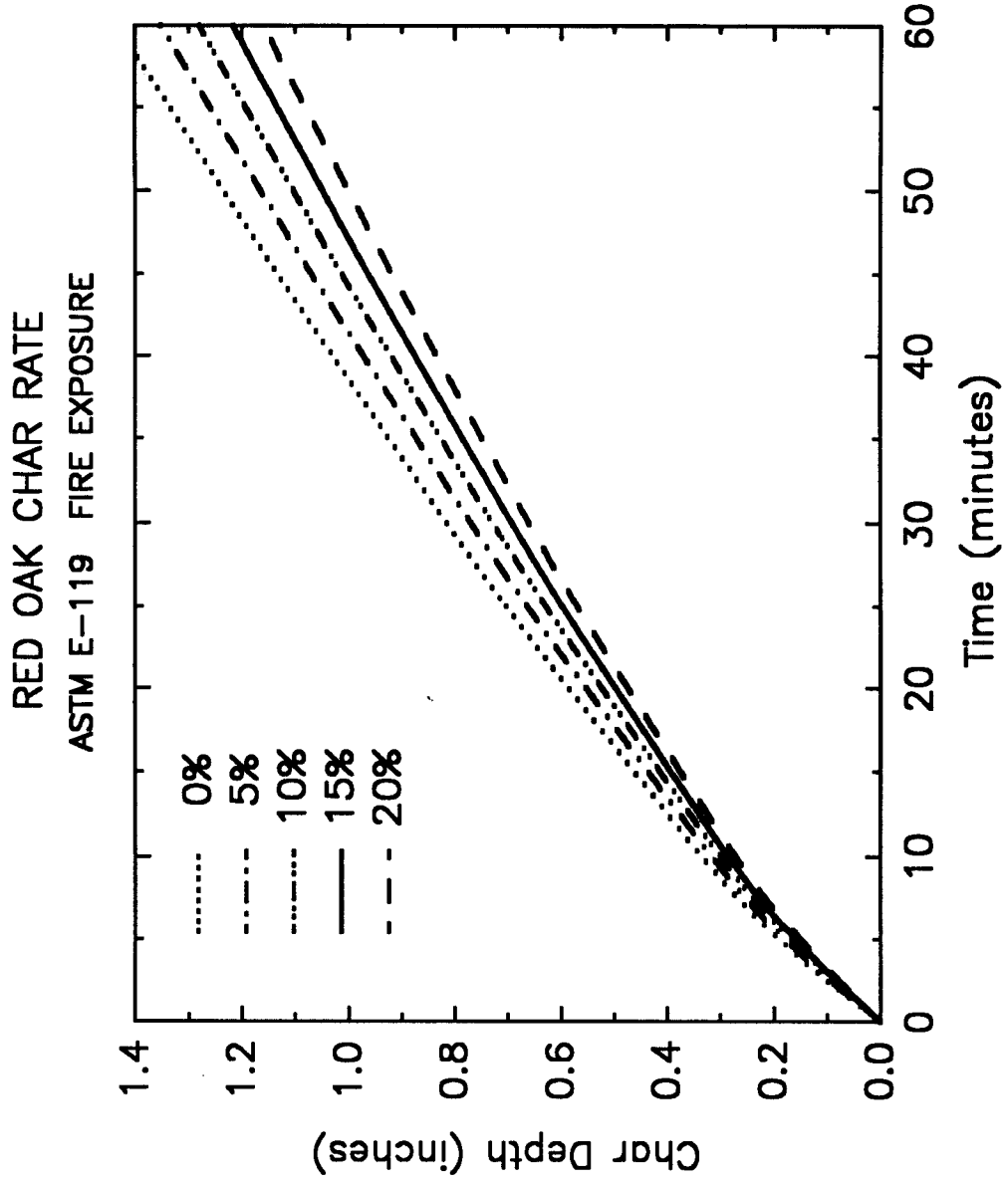

Figure 3.5 Southern pine char rate by White based on ASTM E 119 exposure at various moisture contents.

form:

$$\beta = \frac{q_n}{\rho[C(T_p - T_o) + L_v]} \tag{18}$$

where:
- q_n = net heat flux to uncharred wood
- ρ = density at equilibrium moisture content
- C = specific heat capacity
- T_p = average pyrolysis temperature of wood
- T_o = initial temperature of wood
- L_v = heat of gasification

Experimental charring rate results for pine, spruce, LVL (laminated veneer lumber), plywood, particleboard and fiberboard at various moisture contents are used to verify the relationships. Utilizing the cone calorimeter, three levels of external heat flux, 25kW/m², 50kW/m² and 75kW/m² are applied at constant rates. Unlike previous studies, the location of the char front is at an internal temperature of 360°C, this is in contrast to 288°C established by Schaffer.

Using Equation 18, Mikkola develops relationships between charring rate and external heat flux, density, moisture content and rate of heat release for spruce (ρ = 480 kg/m³, C = 1800 J/kgK, L_v = 1.7 MJ/kg, q_n = 15kW/m², T_p = 360°C, MC = 10%).

External heat flux:

$$\beta = 0.2 q_e + 5 \tag{19}$$

where: q_e = external heat flux (kW/m²)

Figure 3.6 shows the effect of increasing external heat flux on the char rate of spruce.

Density:

$$\beta = \rho^{-1} \tag{20}$$

where: ρ = density of wood sample(kg/m^3)

Mikkola provides an approximate equation for the effect of moisture content on the charring rate. The equation is used to show the relative change in charring rate with a moisture content of 10% normalized.

$$\beta \sim \frac{1}{1+2.5w} \tag{21}$$

$$w=\frac{m-m_o}{m_o} \tag{22}$$

where: w = moisture content
m = mass of wood sample
m_o = mass of dry wood sample

Experimental charring rates from Mikkola, are based on a constant radiant flux to the surface of the wood sample.

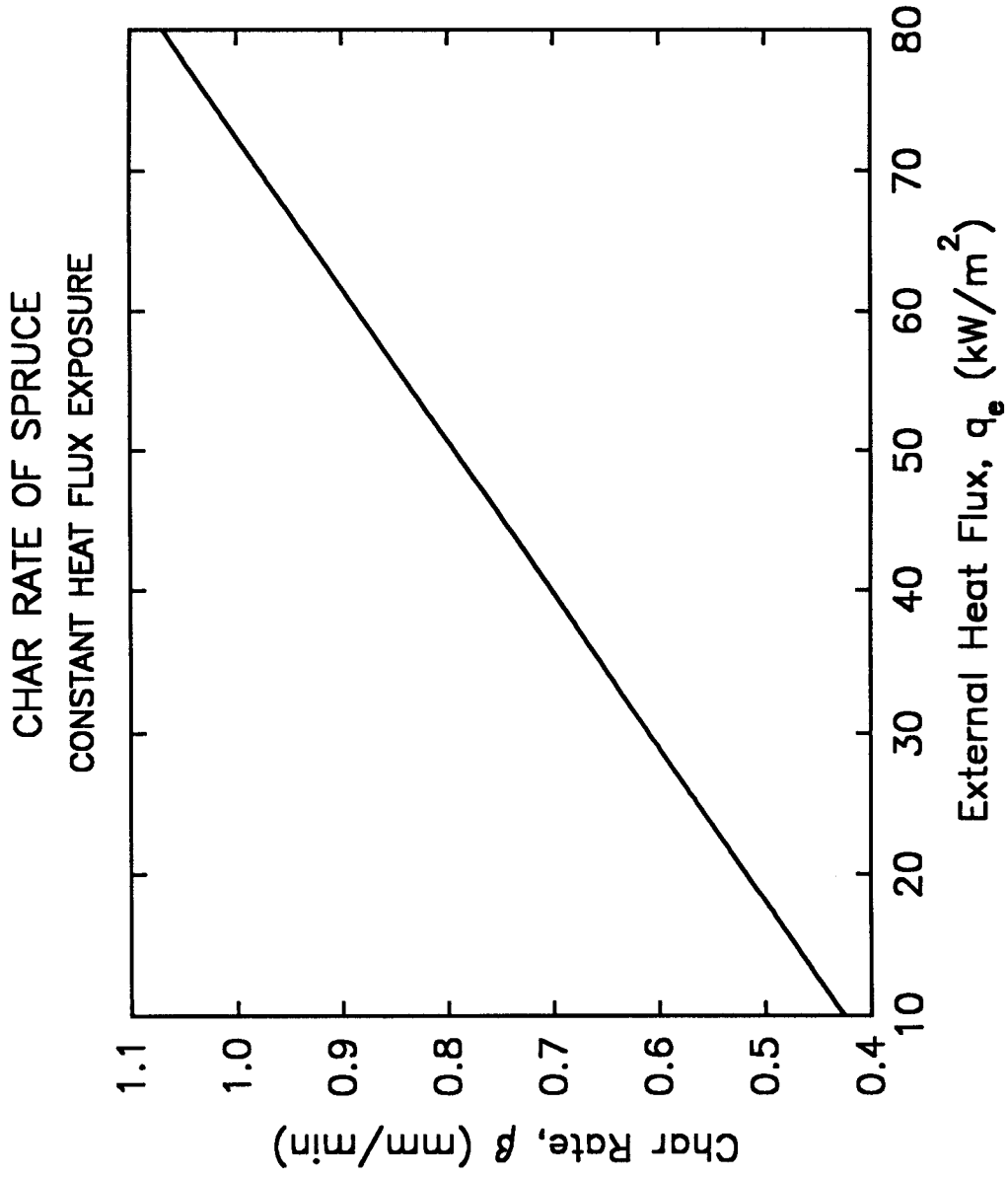

Figure 3.6 Char rate of spruce by Mikkola.

TABLE 3.2

CHARRING RATE B (MM/MIN) [IN/HR] AT DIFFERENT MOISTURE CONTENTS WITH AN EXTERNAL HEAT FLUX OF 50KW/M²					
Wood species or product	Density (kg/m³)	Moisture content			
		0%	8%	10%	20%
Pine	560	1.11 [0.47]		0.8 (2.62)	
Spruce	490	1.06		0.8	0.60
LVL	520	1.05		0.82	0.68
Plywood	640	1.44 [0.61]	1.14		
Particleboard	670	1.10	0.97		
Fiberboard	300	2.40 [1.02]	1.8		

3.3. Temperature profile.

Various researchers have studied the physical changes which occur within wood slabs exposed to external heat sources. The effect of charring on material strength is readily apparent by observation. Within the apparently undamaged fibers, there are physical changes which must be quantified in order to evaluate any strength loss. As previously discussed, the location of peak temperature occurrence in uncharred fibers permits the prediction of strength loss.

Schaffer [25] identified a "dwell" or leveling of the time vs. temperature profile curve for any given thermocouple located at a fixed depth in the slab. The dwell is

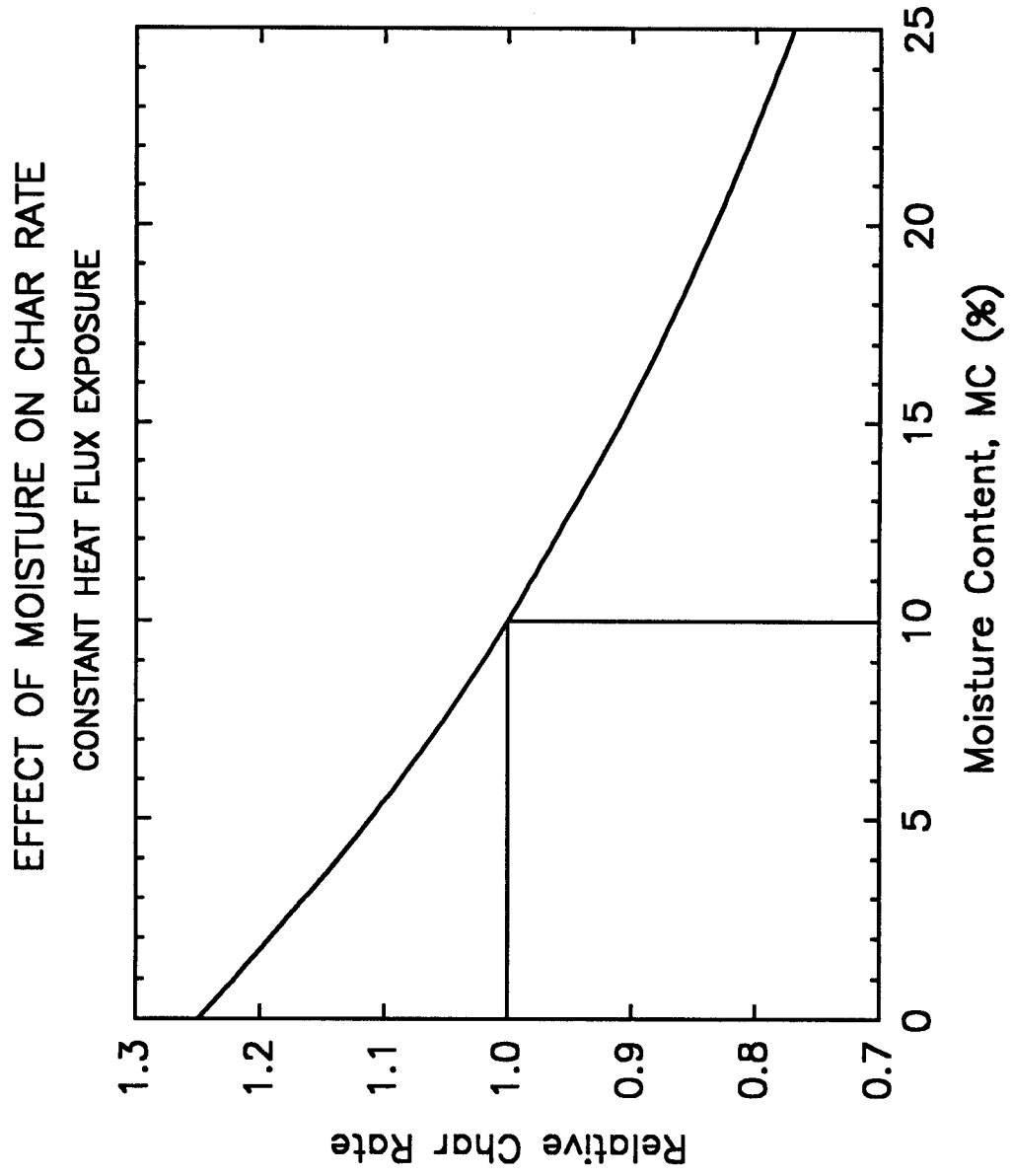

Figure 3.7 Relative char rate normalized by Mikkola.

found to occur consistently at around 100°C, with a steep rise in temperature toward the char front.

Fredlund [33] reports that the depth within the slab at which the temperature is being recorded and the moisture content, affect the length of the dwell. Temperatures were recorded at 2.5, 10, 20, 30, 40, 50, 70, 90, 110, and 130 mm from the specimen surface. Beginning at the 20 mm depth, the temperature profile exhibits the dwell between 100 and 150°C. The length of this dwell is proportional to the depth at which the temperature is recorded. This is a result of water in the liquid phase being vaporized. The effect of moisture content on the temperature gradient can be illustrated by studying oven dry spruce and material with a moisture content of 11.7%. At a 50 mm depth, the oven dry spruce reaches a temperature of 100°C at approximately 9 minutes sooner than the 11.7% moisture content specimen. The presence of moisture retards the heat transfer inward.

Because the fire exposure of ASTM E 119 increases the furnace temperature with time, White concluded that with a constant heat flux, the char rate would slow as the char layer became thicker. Because of the increasing furnace temperature, the affect of the insulative char layer was not as pronounced. This conclusion would suggest that the standard fire curve exposure will produce conservative char rate results. A ventilation controlled fire will maintain a steady temperature, rather than an increasing temperature.

Fredlund studied a number of parameters in the pyrolysis of spruce, pine and chipboard. Experiments were performed on cubes with a dimension of 135mm (5.315 in.) conditioned to an initial moisture content of 0, 12% or 24%. The cubes were insulated with mineral wool on four sides to simulate one dimensional heat flow. The top surface was exposed to a conical radiant panel of constant radiation equal to 75 or 90 kW/m^{-2}. Cubes were exposed for a 60 minute duration, with the results being utilized for modeling purposes.

3.4. Pressure profile.

The movement of moisture away from the char front is a result of higher internal pressure nearer the heat source. The pressure is most likely a result of vaporization of the moisture.

Fredlund reported that reliable pressure measurements were subject to cracks and fissures in the specimens char layer. Fredlund does conclude that the specimens with initial higher moisture contents will produce greater internal pressures. For the materials tested, the spruce and pine exhibited similar internal pressures while the chipboard pressures were lower.

Density recordings at numerous surface distances failed to show moisture accumulation as expected. This was attributed to two possible causes; 1) moisture

insulation was not thoroughly achieved and 2) the instrumentation lacked the sensitivity to record the slight changes in density due to moisture accumulation. The bulk density of the char for each specimen was obtained from the experiments. Results indicated a bulk density (kgm^{-3}) for pine, spruce and chipboard of 150-200, 100-120 and 200-250, respectively.

3.5. Moisture profile

White and Schaffer [30], performed eight tests to study time-moisture content and time-temperature curves in fire exposed wood slabs. Three species of wood were tested, white oak, Douglas-fir and southern yellow pine. White oak and Douglas-fir slabs were exposed to a time-temperature as prescribed by ASTM E 119. The southern yellow pine slab was exposed to three fires; 1) ASTM E 119, 2) 927°C and 3) 538°C.

Results indicate that a linear relationship exists between the time of peak moisture content and the charring rate. The charring rate is defined as the char/wood interface temperature of 288°C. The peak moisture front preceded the 288°C temperature movement in a linear fashion throughout the duration of the tests.

The dwell in the time-temperature curve occurred simultaneously with an increase in moisture content. The average peak moisture content occurred at 98°C with a decrease in moisture content at or above 100°C. The length of the temperature

curve dwell was linearly correlated to the area under the time-moisture content curve following the initial rise in moisture content. It was found that the duration of the dwell in temperature increased, as the area under the time-moisture curve increased, following the initial moisture content increase.

The flow of moisture in the fire exposed slab was attributed to three factors: 1) moisture concentration gradient, 2) temperature gradient and 3) pressure gradient. White and Schaffer are quick to eliminate factors 1 & 2 as primary contributors. They believe that a pressure gradient results from the vaporization of water within the slab. A major variable is the amount of vapor which moves through the slab. This is related to the permeability of the species. The southern yellow pine, which has high permeability, exhibited the highest peak moisture content as well as the greatest fraction of moisture transferred to the cold side of the slab. Likewise, the Douglas-fir heartwood and oak heartwood exhibit less permeability and had lower peak moisture contents.

CHAPTER 4

UNPROTECTED FLOOR JOISTS

4.1. Introduction.

The testing of unprotected joist floor assemblies under ASTM E 119 fire conditions and real fire exposure, has produced fairly accurate methodologies for predicting structural failure times based upon various time-temperature relationships. Although the ASTM E 119 fire exposure is intended for evaluating the relative performance of protected assemblies, the time vs. temperature curve has been used extensively with unprotected assemblies.

The *National Grading Rules for Dimension Lumber* define structural joists as having dimensions of 2-4" thick, 5" & wider. The term "joist" is used to define the lumber which supports floor and ceiling loads, whereas, "rafter" defines the lumber supporting roof loads. Typically, in lightweight wood frame construction, joists sizes of 2" x 8", 2" x 10" and 2" x 12 are common. Rafters include these sizes as well as 2" x 6", depending on load and span. In accordance with the *National Grading Rules*, the term joist will be used to describe both floor and roof members.

Joist framing systems generally consist of numerous parallel structural elements having center to center spacings of 16 or 24 inches. Structural panels span between the underlying joists and effectively transfer the load to the joist. The system effect of a floor

assembly contributes to its fire performance. Significant research has been performed on the behavior of unprotected joist assemblies when exposed to fire.

4.2. Review of historic methodologies.

Lawson [34] performed early work in the development of an empirical model to predict joist failure when exposed to fire. The results of this work are somewhat limited because of the relatively small scale of the test assemblies. In each case, two parallel joists were connected with wood boards in a herringbone strut configuration. The strutting was not assumed to transfer load from the stronger joist to the weaker joist, as is commonly expected due to load sharing. Joist dimensions of 1" x 7", 2" x 6", 2" x 7" and 2" x 9" were utilized. The empirical model derived by this work is represented as:

$$r^{1/2}=0.5(1-T\sqrt{S})(1-0.5T\sqrt{S})^2 \qquad (23)$$

where:
- r = total applied load/breaking load or f_b under applied load/f_b ultimate
- s = depth/breadth
- T = t/20 x $a^{1/4}$
- t = fire endurance, min.
- a = area of cross section, in^2

Son [35] performed tests on two unprotected floor ceiling assemblies of Douglas-fir utilizing 2" x 8" and 2" x 10" joists. The joists were subjected to the ASTM E 119 [36] fire exposure. Times to failure were 13.00 minutes for the 2" x 8" joists and 11.68 minutes for the 2" x 10" joists. In each case, the joists were loaded to 100% of allowable design loads.

The National Forest Products Association [37], [38], [39], [40] sponsored 4 floor joist assembly tests of varying configuration. The unprotected floor joist assemblies were exposed to the ASTM E 119 fire test curve. Two floor systems utilizing joist dimensions of 2" x 8" and 2" x 10" respectively, were sheathed with 23/32" plywood panels with two floor covering treatments. The joists were either Douglas-fir or southern pine, 2" x 8" and 2" x 10" respectively, both with a single member F_b = 1200 psi, according to the 1971 *NDS*® supplement [41] . Since the assembly consisted of multiple joists, the F_b was increased 15% for repetitive member use. This resulted in a maximum allowable F_b = 1450 psi, after rounding. Maximum bending moments were based on a section modulus (S) of 13.141 in^3 for the 2" x 8" and S = 21.391 in^3 for the 2" x 10". Assemblies were loaded to achieve 100% maximum allowable bending moment, are reported in Table 4.1, along with the construction parameters and test results.

Woeste and Schaffer [42], developed a risk based methodology for determining the time to failure under fire conditions of a solid sawn joist system. Time to rupture of the first, second and third joists were recorded. ASTM E 119 test failure occurs when one of three end point criteria are reached, one being structural collapse of the assembly. For the purpose of evaluating unprotected assemblies, Woeste and Schaffer elected to define failure only in terms of structural collapse. The risk based approach considered structural integrity of the floor as the appropriate end point. This condition of failure was intended to address the needs of fire service personnel performing search and rescue, provided the environment above the floor is suitable for such activities.

Woeste and Schaffer developed a model to predict the time to failure of floor joists. Empirical results from Lawson and Son were used to define the parameters of the equation. The Lawson test results provided the primary input data for the derivation of the model. As previously discussed, the Lawson tests assemblies did not provide for load sharing between joists. The 1991 *NDS* defines repetitive members as being "three or more parallel members, connected by structural sheathing, providing continuous bracing of the compression edge".

The flexure formula, $F_b = Mc/I$, was chosen to provide the basis for the probability equation. The effect of cross-sectional area reduction, due to charring, and the loss of fiber strength, due to temperature increases, are accounted for in the model. Utilizing the floor test results from Lawson, with a least-squares nonlinear regression analysis, the following expression provided a good model:

$$\frac{M(d-Ct_f)/2}{(b-2Ct_f)(d-Ct_f)^3/12} = \frac{B}{\frac{1+(b+2d)}{bd}\gamma t_f} \qquad (24)$$

where:
- M = applied bending moment (ft-lb)
- d = joist depth (in.)
- C = char rate (in./min.)
- t_f = time duration of fire (min.)
- B = joist MOR (psi)
- b = initial joist width (in.)
- γ = fire performance factor

A close look at equation 24 reveals a complex flexural formula. The left side of the equation accounts for the loss of the cross sectional area over time due to charring.

At some time t_f, the depth of the joist has been reduced by the value (Ct_f). A reduced depth and moment of inertia, $I = bd^3/12$, account for the effect of charring.

The expression in the denominator of the right side of the equation was chosen after performing a least-squares nonlinear regression analysis on 5 possible expressions for predicting the time to failure. A value of γ equal to 0.170 in./min. was used in the selection of the model given in equation 24.

Solving this equation for t_f yields:

$$t_f = \frac{2Cd(d+b)+6MK\gamma/B-\sqrt{2Cd(d+b)+6MK\gamma/B^2-4V^2(b+d)(bd^2-6M/B)}}{2C^2(b+4d)} \quad (25)$$

where:

$$K = \frac{(b+2d)}{bd} \quad (26)$$

The equation was validated against the series of 4 unprotected floor joist fire test conducted by the National Forest Products Association. While the analytical results produce an earlier time to failure than the NFPA tests, a number of factors are influential. Most notably, the Lawson tests were conducted with only two joists per assembly while the NFPA tests resembled a typical repetitive joist floor framing system. Also, joists in the NFPA test were sheathed with plywood subflooring. This delayed failure of the

joists.

Because the fire test results which were utilized to determine the mathematical model expressed by equation 24 differed from NFPA tests, only partial comparisons are possible.

TABLE 4.1

PREDICTED AND ACTUAL TIMES TO FAILURE FOR NFPA UNPROTECTED FLOOR FIRE ENDURANCE TESTS

Sample	Nom. Size	Applied joist moment	B eq. 25	C eq. 25	Predicted t_{r1}	Assembly Observed t_r	Joist Observed t_r
		In. lb	lb/in^3	In./min.	Minutes	Minutes	Minutes
No.2 Douglas-fir "S-dry" w/vinyl tile, 19/32 in. plywood.	2 x 8	19,054	4308	0.0245	5.42	10.2	5.0
No. 2 Douglas-fir "S-dry" w/nylon carpet, 19/32 in. plywood.	2 x 8	19,054	4308	0.0245	5.42	12.86	11.5
No. 2 MG southern pine "S-dry" w/vinyl tile, 23/32 in. plywood.	2 x 10	31,017	5730	0.03	7.01	13.34	9.0
No. 2 MG southern pine "S-dry" w/nylon carpet, 23/32 in. plywood.	2 x 10	31,017	5730	0.03	7.01	12.06	12.06

White, R. H., Schaffer, E. L. and F. E. Woeste [43] performed testing on Douglas-fir floor joist assemblies. The purpose of the testing was to develop further empirical results to refine γ, the exposed joist performance factor. Eleven floor tests assemblies were subjected to the ASTM E 119 fire exposure, with superimposed live loads of 11.35

#/ft^2 and 79.2 #/ft^2. These two loading levels were selected since 11.35/ft^2 was reported by [44] to be the mean live load in one and two family dwellings and 79.2#/ft^2 represents full design load.

The sheathing for the tests was selected to be 23/32" tongue and groove plywood. Because of the concern for failure due to burn through of the plywood prior to joist failure, a small scale test consisting of two joist was conducted. Results from this test using an 11.35 #/ft^2 live load assured them that joist failure would occur before plywood burn through.

Each floor assembly consisted of 12, 2" × 10" joists spanning 13'6". The results are given in Table 4.2. As the failure times indicate, the percentage of full design load applied is critical in approximating the time to failure. Based on linear interpolation between the two loads tested, Woeste and Schaffer predict a time to failure of 13.1 minutes for a 40 #/ft^2 live load. This particular live load is typical of a minimum design load required by the building codes for a single family dwelling unit. Lie [45] would suggest that a linear interpolation between points is inappropriate as fire endurance increases at a nonlinear rate.

In 1980, Fang [46] performed tests on 2 assemblies of unprotected solid sawn joists. Unlike previous floor tests utilizing the ASTM E 119 fire exposure, a "real fire" exposure was chosen. The fire load was provided by a sofa, chair, end table, bookcase,

TABLE 4.2

OBSERVED TIMES-TO-FAILURE OF WOOD JOISTS.

Floor no.	Live load level	First joist failure		Second joist failure		Third joist failure	
		Joist no.	Time	Joist no.	Time	Joist no.	Time
	lb/ft^2		mins.		mins.		mins.
Trial	11.35	2	16.7	7	17.0	8	17.0
1	11.35	5	17.8	7	18.0	3	18.5
2	11.35	5	16.8	4	17.2	3	17.4
3	11.35	4/5	18.0	4/5	18.0	2	18.5
4	11.35	6	18.4	7/9	18.8	7/9	18.8
5	11.35	6	18.5	6/7	18.5	8	18.9
mean			17.9		18.1		18.4
6	79.2	5/6	6.2	5/6	6.2		
7	79.2	12	6.8	8/9	7.6	8/9	7.6
8	79.2	3/5	7.5	3/5	7.5	7	7.7
9	79.2	6	5.5	7	5.6	9	6.3
10	79.2	6	6.3	7	6.7	9	6.8
mean			6.5		6.7		7.1

1) Coefficients of variation of results are 3.7%, 3.2% and 3.2% for first, second and third joist failures, respectively.
2) Coefficients of variation of results are 11.6%, 12.4% and 9.4% for first, second and third joist failures, respectively.

coffee table and loose paper. The fire growth curve which resulted from this fuel package, was intended to reflect a typical fire growth consisting of the initial phase, flashover, full room involvement and the decay period.

Failure of the assembly was defined as structural failure, which included excessive deflection or the passage of flames or hot gases to the unexposed surface. The

unprotected assemblies consisted of 2" x 8" joists on 16" and 24" spacings, with an applied load of 40 lb/ft^2, which resulted in maximum allowable stresses of 69% and 100%, respectively. Plywood subflooring of 5/8" was used on the 16" spacing and 23/32" was used on the 24" spacing.

The assembly with 16" joist spacing failed due to rupture of a centrally located joist at 10 min: 43 sec. Prior to this time, flame penetration had occurred through the plywood subfloor. The assembly with 24" joist spacing failed due to joist rupture at 12 min: 0 sec. The rate of deflection increased rapidly just prior to the first joist failure.

In 1983, Fang [47] performed additional testing of floor assemblies using protected and unprotected, solid sawn joists. The emphasis on this testing was to finalize a proposed fire exposure curve similar to that used in 1980. Parallel tests were performed between the proposed curve and the ASTM E 119 exposure, utilizing identical assembly construction methods.

The work of White and Schaffer, as previously discussed, provided suitable experimental data for the validation of the model developed by Schaffer and Woeste. White, Schaffer and Woeste [48], performed a validation and refinement of the earlier work. One of the more significant recommendations, results in a change of the exposed joist factor, γ, from 0.17 to 0.20. This increase was justified based upon, "improved confidence in the control of the materials used and testing conducted in this study

[1983]". Equation 25 provided predicted times to failure within one standard deviation of the actual time to failure of the 1983 tests results. Additionally, the sensitivity of the model to a number of parameters was checked, which resulted in the following conclusions:

> "An exponentially decreasing effect on time to failure of increasing load."

Comment: As incremental increases to load are made to lighty stressed joists, time to failure increases are larger (time to failure is sensitive to load). As incremental increases are made to high loads, there is little change in the time to failure (time to failure is insensitive to load)

> "High sensitivity to char rate when floors are under low load, but insensitivity at high loads."

Comment: Lightly loaded joists will resist failure even after significant loss of the cross-section due to charring. The rate at which this charring occurs affects the time to failure. Likewise, heavily loaded joists will fail after the loss of little cross section, therefore, the rate of charring is not significant, since the time to failure is relatively short.

> "High sensitivity of time to failure to the strength of the joists (MOR) (that is, the higher the actual joist strengths are compared to design strengths, the longer the time to failure)."

Comment: Because of the safety factor associated with the 5th percentile exclusion value, actual joist strength generally exceeds design strength. Therefore, the closer the assumed strength of the joist is to the actual strength, the more closely time to failure can be predicted.

> "Insensitivity of time to failure to joist depth, but increase of time to failure with increase in width."

Comment: At narrow widths, typical of floor joists, the loss of cross section width is significant in contributing to failure, whereas difference in joist depth is not. Increasing the joist width will cause the width to become less sensitive, while causing differences in joist depth to become more sensitive.

CHAPTER 5

PROTECTED FLOOR/CEILING ASSEMBLIES

5.1. Introduction.

As discussed in Chapter 4, unprotected wood frame assemblies have predictable performance under fire exposure. Models have been developed to allow for comfortable results to be predicted. The same is not true for protected assemblies. Presently, there are no models available to predict the time to failure of protected assemblies. The identification of gypsum board physical properties by Mehaffey [49], will allow for the development of models for protected assemblies.

There are two methods currently available for gaining acceptance of a rated assembly. The most recognized is by testing the assembly in accordance with the ASTM E 119 fire test standard. Alternatively, for typical wood-frame wall and floor assemblies, the *Component Additive Method* (CAM) [50] allows various membrane products to be combined with structural elements, to achieve a desired rating time. Both methods are discussed further in this chapter.

5.2. The role of rated assemblies.

The building codes distinguish between buildings which are constructed of "protected or rated" assemblies and those which are of "unprotected" construction.

Buildings of protected construction are permitted to be larger in allowable floor area and have more stories. The following table illustrates the impact on the area and height of protected, Type 5 construction in the National Building Code. Buildings constructed wholly or partially of wood frame construction are considered Type 5 construction.

TABLE 5.1

Use Group	Type 5A Protected	Type 5B Unprotected
A-1 - Assembly, theaters	1 St. 20' 8,925	1 St. 20' 4,200
B - Business	3 St. 40' 15,300	2 St. 30' 7,200
H - High Hazard	1 St. 20' 5,100	NOT PERMITTED
M - Mercantile	2 St. 30' 10,200	1 St. 20" 4,800

The design professional is in a position to determine the most economical type of construction for a proposed building. If the building height and area complies with the unprotected limitations, there is no real building code incentive to provide protected assemblies.

5.3. Present practice.

The ASTM E 119 time vs. temperature curve was first published in 1918. Since then, test procedures have been periodically updated. The ASTM E 119 fire test is

recognized today in the model building codes as the standard for fire rated assembly acceptance. Due to this long history, there have been a large number of tests conducted on wood frame assemblies utilizing various methods of membrane protection.

5.4. Test results.

Historically, design professionals have relied on published results of tests which are conducted at qualified testing laboratories. The results are published in a number of documents including the Underwriter's Laboratory Fire Resistance Directory [51], Warnock Hersey Fire Resistance Directory [52] and the Gypsum Association Directory of Rated Assemblies [53]. More recently, with the introduction of specialty products, assembly ratings are often provided as part of the manufacturer's National Evaluation Report.

5.5. ASTM E 119 examples.

Grundahl [54], provided a review of ten reports containing seventeen (17) assemblies which used lightweight structural elements and a single layer gypsum membrane. The structural elements used in the assemblies are either metal toothplate connected wood trusses or steel joists. Grundahl concludes that in general, if the assembly depth is in excess of 10" and a single layer of 5/8" Type C gypsum board is attached to the structural element, a rating of 45 minutes is expected.

The *UL Directory* provides a listing of approximately 50 floor/ceiling assemblies using solid sawn wood joists or parallel chord trusses. Variations in the type of membrane protection, i.e. gypsum wallboard or suspended ceiling and floor toppings/coverings, contribute to the many choices.

The Warnock Hersey *Listings* contain approximately 30 floor/ceiling assemblies. Many of the assemblies use engineered wood products such as I-joists or metal web trusses. Assigned fire endurance ratings range from 45 minutes to 1 hour.

5.6. Component additive method.

The Component Additive Method (CAM) has its origin dated to tests performed at the British Fire Research Station between 1945 and 1946 as reported by Lawson, Webster and Ashton [34]. In the report of the Associate Committee on the National Building Code, National Research Council (NRC), Canada (date unknown), the conclusion of Lawson, et al, states:

> "it has been found by experience that the large majority of floors exposed to fire failed by collapse of a wood joist floor, time to failure can be predicted by adding together -
>
> (1) the time for fire (to) penetrate the ceiling, and
>
> (2) the calculated time to failure of the wood joist based on,

rate of burning, and ratio of applied load to breaking load."

Prior to 1946, the ASTM E 119 test criterion stated failure of a wood assembly occurred when the surface of the wood reached 250°F. Since then, fire is allowed to reach the joists and 250°F can be exceeded. The 250°F interior temperature is similar to the UL listing of a finish rating. Recognizing that this failure criterion was inappropriate, the NRC began a program of analyzing the results of ASTM E 119 and BS 476 testing, to determine trends in failure times of wood joist floor systems with and without protective membranes. The results of this effort, combined with the British report, provided the basis for the Canadian CAM. The most significant contribution from the British report, is the assigned value of 10 minutes for floor joists. The Canadian report incorporated an additional time for the use of mineral wool insulation.

This procedure has led to the adoption of the CAM in the *UBC* [55] and the *SBC* [56] as an option for compliance with required fire endurance ratings. The procedure to determine the fire endurance of a wall or floor/ceiling assembly requires identification of the assembly components. Each component is listed individually as to its assigned time. The times of each component are cumulative with the sum equal to the assigned fire endurance rating.

The methodology resulted from a detailed review of 135 standard fire test reports on wood stud walls and 73 test reports on wood-joist floor assemblies and the *Ten Rules*

of Fire Endurance Rating by Harmathy [57]. Review of the fire tests provided assigned time values for contribution to fire endurance ratings for each separate component of an assembly. The "Ten Rules" provided a method for combining the individual contributions of the elements to the overall fire endurance rating of the assembly.

The following CAM procedures were prepared by the author. Examples and illustrations are provided by permission of the American Forest & Paper Association and can also be found in their publication on this topic [50].

DESIGN PROCEDURES

Wood frame assemblies: Fire resistance ratings up to 1-hour duration are permitted to be calculated for walls, floor/ceiling and roof/ceiling assemblies, by combining the individual component times of the assembly in accordance with this section. The calculated time shall equal or exceed the required fire resistance rating of the assembly.

Calculating fire endurance: The fire resistance rating of a wood framed assembly is equal to the sum of the time assigned to the membrane on the fire exposed side, Table 5.2, the time assigned to the framing members, Table 5.3 and the time assigned for additional contribution by cavity insulation, Table 5.4. The membrane on the unexposed side shall not be included in determining the fire resistance of the assembly.

TABLE 5.2

TIME ASSIGNED TO PROTECTIVE MEMBRANES	
Description of Finish[a,b]	Time (min)
3/8 inch Douglas fir plywood, phenolic bonded	5
½ inch Douglas fir plywood, phenolic bonded	10
5/8 inch Douglas fir plywood, phenolic bonded	15
3/8 inch gypsum board	10
½ inch gypsum board	15
5/8 inch gypsum board	20
½ inch Type X gypsum board	25
5/8 inch Type X gypsum board	40
Two layers 3/8 inch gypsum board	25
One layer ½ plus one layer 3/8 inch gypsum board	35
Double ½ inch gypsum board	40

Note a: On walls where only plywood is used as the fire exposed membrane, the cavity shall be insulated with any of the insulations listed in Table 5.4

Note b: On walls, gypsum board shall be installed with the long dimension parallel to framing members with all joints finished. 5/8" gypsum board is permitted to be installed horizontally with the horizontal joints unsupported. On floor/ceiling or roof/ceiling assemblies, gypsum board shall be installed with the long dimension perpendicular to framing members and shall have all joints finished.